Published Online First on March 2, 2010 as 10.1158/0008-5472.CAN-09-2661

Molecular and Cellular Pathobiology

Cancer Research

p53 Regulates the Ras Circuit to Inhibit the Expression of a Cancer-Related Gene Signature by Various Molecular Pathways

Yosef Buganim[1], Hilla Solomon[1], Yoach Rais[1], Daria Kistner[1], Ido Nachmany[1], Mariana Brait[3], Shalom Madar[1], Ido Goldstein[1], Eyal Kalo[1], Nitzan Adam[1], Maya Gordin[1], Noa Rivlin[1], Ira Kogan[1], Ran Brosh[1], Galit Sefadia-Elad[2], Naomi Goldfinger[1], David Sidransky[3], Yoel Kloog[2], and Varda Rotter[1]

Abstract

In this study, we focus on the analysis of a previously identified cancer-related gene signature (CGS) that underlies the cross talk between the p53 tumor suppressor and Ras oncogene. CGS consists of a large number of known Ras downstream target genes that were synergistically upregulated by wild-type p53 loss and oncogenic H-Ras^{G12V} expression. Here we show that CGS expression strongly correlates with malignancy. In an attempt to elucidate the molecular mechanisms underling the cooperation between p53 loss and oncogenic H-Ras^{G12V}, we identified distinguished pathways that may account for the regulation of the expression of the CGS. By knocking-down p53 or by expressing mutant p53, we revealed that p53 exerts its negative effect by at least two mechanisms mediated by its targets B-cell translocation gene 2 (BTG2) and activating transcription factor 3 (ATF3). Whereas BTG2 binds H-Ras^{G12V} and represses its activity by reducing its GTP loading state, which in turn causes a reduction in CGS expression, ATF3 binds directly to the CGS promoters following p53 stabilization and represses their expression. This study further elucidates the molecular loop between p53 and Ras in the transformation process. *Cancer Res; 70(6); 2274–84. ©2010 AACR.*

Introduction

Two of the most pivotal players in the malignant process are the tumor suppressor p53 and the proto-oncogene Ras (1, 2).

p53 is a transcription factor that, under basal conditions, is found at low levels due to its negative regulator HDM2 (3, 4). Following stress signals, p53 is stabilized leading to induction of multiple cell responses, such as cell cycle arrest, apoptosis, and DNA repair (5). p53 stabilization is critical for tumor development prevention; therefore, the majority of human cancers exhibit a high incidence of p53 dysfunction, manifested by changes in p53 expression, mutation of the p53 protein, or indirect modification of other p53 pathway components (6).

At least three major pathways have been suggested to account for the accumulation of p53 in response to stress signals: the DNA damage pathway, the Jun-NH_2 terminal kinase 2 pathway, and the oncogenic stress-induced pathway, which is often triggered by oncogenic Ras (7).

Members of the Ras family of GTPases play a central role in cell proliferation and survival; therefore, aberration in the Ras pathway may lead to neoplastic transformation (8). Three pivotal Ras genes are encoded in the human genome: *H-Ras, K-Ras,* and *N-Ras*. Ras activation is controlled mainly by two enzyme families: the guanine nucleotide exchange factors (RasGEF), which induce GDP to GTP exchange leading to Ras activation, and the GTPase activating proteins (RasGAP), which facilitate GTP hydrolysis that convert Ras into its inactive form. The Ras proto-oncogene can be constitutively activated in a variety of human tumors by point mutations that render it less sensitive to RasGAPs (1). The active Ras protein induces downstream signaling cascades, including the mitogen-activated protein kinase (MAPK), phosphatidylinositol 3-kinases (PI3K), and RAL guanine nucleotide dissociation stimulator cascades (9), which contribute to tumorigenesis.

The fact that both the tumor suppressor p53 and the Ras proto-oncogene are highly mutated in human cancers prompted us to revisit the notion that these counteracting key proteins are engaged in a specific yet uncovered molecular cross talk along the transformation process.

Pioneering studies have shown that coexpression of active H-Ras^{G12V} (H-Ras^{V12}) together with mutant p53 resulted in the induction of aggressive transformed phenotypes (10–12). Recently, it has been found that H-Ras^{V12} and p53 knockdown synergistically induce RhoA activity, leading to increased cell motility (13). Moreover, p53 has been suggested to regulate the levels of a specific *H-Ras* splice variants (14). Other studies

Authors' Affiliations: [1]Department of Molecular Cell Biology, Weizmann Institute of Science, Rehovot, Israel; [2]Department of Neurobiochemistry, George S. Wise Faculty of Life Sciences, Tel-Aviv University, Tel-Aviv, Israel; and [3]Department of Otolaryngology-Head and Neck Surgery, Johns Hopkins University School of Medicine, Baltimore, Maryland

Note: Supplementary data for this article are available at Cancer Research Online (http://cancerres.aacrjournals.org/).

Y. Buganim and H. Solomon contributed equally to this study.

Corresponding Author: Varda Rotter, Department of Molecular Cell Biology, Weizmann Institute of Science, Rehovot 76100, Israel. Phone: 972-8-9344070; Fax: 972-8-9465265; E-mail: varda.rotter@weizmann.ac.il.

doi: 10.1158/0008-5472.CAN-09-2661

suggested that activating transcription factor 3 (ATF3) and B-cell translocation gene 2 (BTG2), two known p53 target genes, suppress Ras-induced transformation by repressing *cyclin D1* expression, leading to growth arrest (15, 16).

In our previous study wherein we established a stepwise *in vitro* model for malignant cell transformation, we identified a unique gene cluster consisting of procancerous secreted molecules, designated here as cancer-related gene signature (CGS), that is synergistically expressed following inactivation of p53 by the dominant-negative peptide GSE56 and by the expression of oncogenic H-Ras^{V12}. Importantly, this cluster was predominantly expressed in cells proficient in developing tumors (17, 18). In agreement with these observations, it has been shown recently that a large proportion of genes controlled synergistically by loss of p53 function and Ras activation harbors promalignant activities (19, 20).

Nevertheless, the question of how inactivation of p53 synergizes with oncogenic Ras^{V12} in the induction of tumorigenesis remained largely unknown.

In this study we show that the cross talk between p53 and Ras^{V12} involves the expression of the CGS. We found that p53 inactivation induces the Ras^{V12} pathway through diverse mechanisms involving the p53 targets BTG2 and ATF3. This in turn facilitates the malignant transformed phenotype of cells, which was accompanied by the accentuated expression of CGS.

Materials and Methods

Cell lines. The Phoenix retrovirus–producing and the H1299 non–small cell lung carcinoma cells were obtained from American Type Culture Collection. Immortalized WI-38 embryonic lung fibroblast cells, immortalized EP156T prostate epithelial cells, and immortalized PM151T prostate smooth muscle cells were established and maintained as described (17, 21). Human umbilical vein endothelial cells (HUVEC) were obtained from PromoCell.

Transfections, infections, and treatments. Infection procedures were conducted as described (17). Transfections were conducted using Lipofectamine-2000 (Invitrogen). Knockdown of ATF3 and BTG2 was conducted by transfection with specific oligo-nucleotides using DharmaFECT3 (Dharmacon). The analysis was performed 72 h posttransfection. PD-98059 (10 μmol/L) and LY-294002 (25 μmol/L) treatment was conducted at 80% confluency. DMSO was used as a control.

RNA isolation and quantitative real time-PCR. Total RNA was isolated using NucleoSpin kit (Macherey-Nagel). A 2-μg aliquot of the RNA was reverse transcribed using Bio-RT (BIO-LAB) and random hexamer. Quantitative real-time PCR (QRT-PCR) was done with ABI7300 instrument (Applied Biosystems) using Platinum SYBR Green qPCR SuperMix (Invitrogen). The values for specific genes were normalized to glyceraldehyde-3-phosphate dehydrogenase (*GAPDH*). Primer sequences are provided in Supplementary Table S1.

CXCL1 and interleukin-1β ELISA and matrix metalloproteinase 3 zymography assays. Cells were grown on six-well plate with serum-free MEM for 72 h. Cell conditioned media were collected, and CXCL1 and interleukin-1β (IL-1β) proteins were detected using the human GRO-α/CXCL1 or IL-1β immunoassay kit (R&D Systems) according to the manufacturer's instructions. For matrix metalloproteinase 3 (MMP3) protein detection, cell media were separated on gelatin-containing polyacrylamide gels. Gels were incubated overnight in developing buffer (430AG-6, Sigma), in 37°C, for MMP enzymes activation. Gels were stained with Coomassie-blue solution (0.1–0.5% Coomasie-blue brilliant R250 in 5% acetic acid and 10% methanol) to detect catalytic activity.

Subcutaneous tumorigenicity assay. Subcutaneous tumorigenicity assay was conducted as described (17). Tumor size was monitored weekly. Mice were sacrificed when tumors reached 1 cm or after 16 wk. Tumors were collected and minced. Tumor fragments were fixed in 4% paraformaldehyde for histologic examination. Fragments were minced, washed in PBS, and plated in culture media. All mouse procedures were done with the approval of the Animal Care and Use Committee of the Weizmann Institute of Science (Israel).

Ras activity (Ras binding domain) pull-down assay, ATF3 and BTG2 binding assay, and Western blot. The GST-Ras binding domain (RBD) GST-BTG2 and GST-ATF3 fused beads were prepared as described (22). Cells were lysed in cold RBD lysis buffer. Equal amounts of cell extracts were incubated O/N with the GST-RBD, GST-BTG2, GST-ATF3, or GST-Empty beads. The proteins were eluted, separated on SDS-polyacrylamide gels, and analyzed. Western blotting was conducted as described (17).

HUVEC migration assay. Cells were plated on 24-well plates, and media were changed 24 h later. After 36 h, conditioned medium was transferred to the bottom of 24-well plate and 5×10^4 HUVECs were plated on top of 8-μm pore 24-Transwell membrane (Clonetic) for 12 h. HUVECs that were migrated to the Transwell outer side were trypsinized and counted.

Coimmunoprecipitation and chromatin immunoprecipitation analysis. Coimmunoprecipitation and chromatin immunoprecipitation was conducted as described (23). To detect ATF3 or p53 binding to the *CXCL1, IL-1β, MMP3, p21^{WAF1},* and *ATF3* promoters, QRT-PCR was conducted using specific primers (see Supplementary Data).

p53 and K-Ras mutational analysis. After patient deidentification, lung cancer histology slides were reviewed for diagnosis confirmation. Fresh frozen or paraffin-embedded specimens were microdissected to obtain >70% neoplastic cells. DNA was extracted as described (24). RNA was extracted from fresh frozen tissue specimens using the QIAzol lysis reagent (Qiagen). cDNA synthesis was done using random hexamers or oligo(dT) with the SuperScript II Reverse Transcriptase (Invitrogen). The tumor DNA samples were analyzed by direct dideoxynucleotide sequencing, the GeneChip p53 assay (Affymetrix), and automated fluorescent-based sequencing, as described (25). Mutations at codons 12 and 13 of *K-Ras* gene were determined using a mismatch assay as described (26, 27).

For antibodies, compounds, plasmids, and primers, see Supplementary Data.

Results

Knockdown of wild-type p53 or mutant p53^{R175H} overexpression synergizes with H-Ras^{V12} in inducing CGS. Recently, an *in vitro* transformation model was established in our laboratory (17, 18). In this model immortalized WI-38 cells were subjected to several genetic modifications, leading to premalignant phenotypes. To acquire fully transformed phenotypes capable of inducing tumors in mice, a concomitant expression of oncogenic H-Ras^{V12} and GSE56 (p53 inactivator) was required. cDNA microarray analyses revealed CGS, which was of particular interest because it was synergistically upregulated by H-Ras^{V12} and GSE56 and appeared only in cells proficient in developing tumors (17, 18).

The CGS consists mainly of secreted molecules that were shown to promote tumorigenicity and at least part of them induced by activated Ras (28–30). Among them are chemokines, interleukins, ECM-related proteins, and others (Fig. 1A).

This observation prompted us to investigate how inactivation of p53 molecularly cooperates with H-Ras^{V12} to induce CGS. Because inactivation of p53 in tumors achieved by point mutations and to a lesser extent by deletions, we decided to establish additional WI-38 system that better represents the p53 status in cancer. Immortalized WI-38 cells overexpressing H-Ras^{V12} (Ras) or empty Hygro control vector (Hyg) were either knocked down for p53 by specific shRNA (shp53) to recapitulate p53 allelic loss or abnormal degradation by HDM2 or overexpressed a frequent hot spot p53 mutant, p53^{R175H} (Fig. 1B). As a control shRNA against the mouse but not the human NOXA gene (shmNOXA) was used. Next, we compared the levels of 10 CGS genes in the established cells (Supplementary Fig. S1A). Three representative genes from each group of the CGS (chemokines, *CXCL1*; interleukins, *IL-1β*; ECM-related genes, *MMP3*) that were shown to promote tumorigenicity were picked and examined throughout the entire study. In agreement with our previous data, Ras/shp53 or Ras/p53^{R175H} cells exhibited an upregulated expression of CGS both at the mRNA and protein levels when compared with their shmNOXA counterparts (Fig. 1C and D).

To examine how general this phenomenon is, we measured the expression of CGS in other systems that were established in our laboratory (21). We found elevated levels of CGS following overexpression of H-Ras^{V12} and p53 knockdown in two prostate cell systems (Supplementary Fig. S2).

This results show that p53 knockdown or mutant p53 overexpression leads to the augmentation in CGS expression in several cell systems, similar to that observed initially where p53 was inactivated by GSE56 (18).

High CGS levels correlate with malignancy. To confirm that high CGS levels associate with malignancy, we performed an *in silico* comparative analysis using the "ONCOMINE" database. Data obtained indicated a significant upregulated expression of CGS in at least three human tumors (head and neck, ovarian, and seminoma) compared with their normal counterparts (Fig. 2A). Subsequently, we evaluated CGS levels in 22 human lung cancer samples well-characterized for *p53* and *K-Ras* status. Although a low frequency of mutations in both *K-Ras* and *p53* was observed; the strongest expression of CGS was evident in a sample that harbors the mutant form of both *Ras* and *p53* (Fig. 2B).

Next, we measured the capability of Ras/shp53, Ras/p53^{R175H}, and Ras/shmNOXA cells to induce tumors in mice. Each cell line was injected into five mice, and their growth rate was monitored weekly. Whereas Ras/shmNOXA cells did not give rise to tumors, both Ras/shp53 and Ras/p53^{R175H} cells showed 100% incidence of tumor uptake. Pathologic examination determined sarcoma type tumors (Fig. 2C). Interestingly an augmentation in growth characteristics was witnessed in Ras/p53^{R175H} compared with Ras/shp53 cells. This was indicated by an earlier tumor appearance, increased cell density, and a higher mitotic rate. Importantly, when CGS levels were monitored in the Ras/shp53 and Ras/p53^{R175H}-derived tumors, significant augmentation in CGS levels were observed when compared with their parental *in vitro* cells (Fig. 2C). In accordance with their higher aggressive phenotype, p53^{R175H} mutant tumor exhibited the most significant increase in CGS expression, which further support the mutant p53 gain-of-function concept (31, 32). Because the CGS is enriched with factors that were shown to play roles in angiogenesis (33, 34), we decided to examine the capability of the various WI-38 cells to attract endothelial cells through Transwells. Notably, a significant number of endothelial cells were migrated through the Transwell when conditioned media from either Ras/shp53 or Ras/p53^{R175H} cells was used compared with the other control cells (Hyg/shmNOXA, Ras/shmNOXA, Hyg/shp53, and Hyg/p53^{R175H}) and to Ras/shp53 or Ras/p53^{R175H} cells treated with Ras pathway inhibitors (Fig. 2D).

Taken together, these results show a strong association between high CGS levels, p53 loss, H-Ras mutation, and malignancy.

p53 knockdown and p53^{R175H} mutant cells exhibit high H-Ras activity. Because the mRNA levels, the protein levels, and H-Ras localization were comparable in all H-Ras^{V12}–expressed cells (Figs. 1B and 3A; Supplementary Fig. S3), we decided to measure the levels of the active H-Ras fraction (H-Ras-GTP) using the RBD pull-down assay (35). Remarkably, we found that Ras/shp53 and Ras/p53^{R175H} cells exhibited significant higher H-Ras-GTP levels compared with their Ras/shmNOXA counterparts (Fig. 3A). This observation is important due to the fact that H-Ras^{V12} is considered less sensitive to p120RasGAP-induced GTP hydrolysis (36). However, when Scheele and colleagues examined the percentage of the H-Ras-GTP fraction in NIH-3T3 cells overexpressing H-Ras^{V12}, 29% of total H-Ras^{V12} was GTP-bound, indicating that H-Ras^{V12} is still free to bind additional GTPs (37). These results unravel a hitherto unknown tumor-suppressive function for p53, whereby p53 inhibits oncogenic H-Ras^{V12} activity by reducing its GTP loading state. Moreover, the synergistic effect observed in the CGS expression in Ras/shp53 and Ras/p53^{R175H} cells might be explained by the elevation of H-Ras^{V12} activity.

The MAPK and PI3K pathways are involved in the induction of CGS. As the most studied cascades of Ras are MAPK and PI3K (9), we analyzed their involvement in the

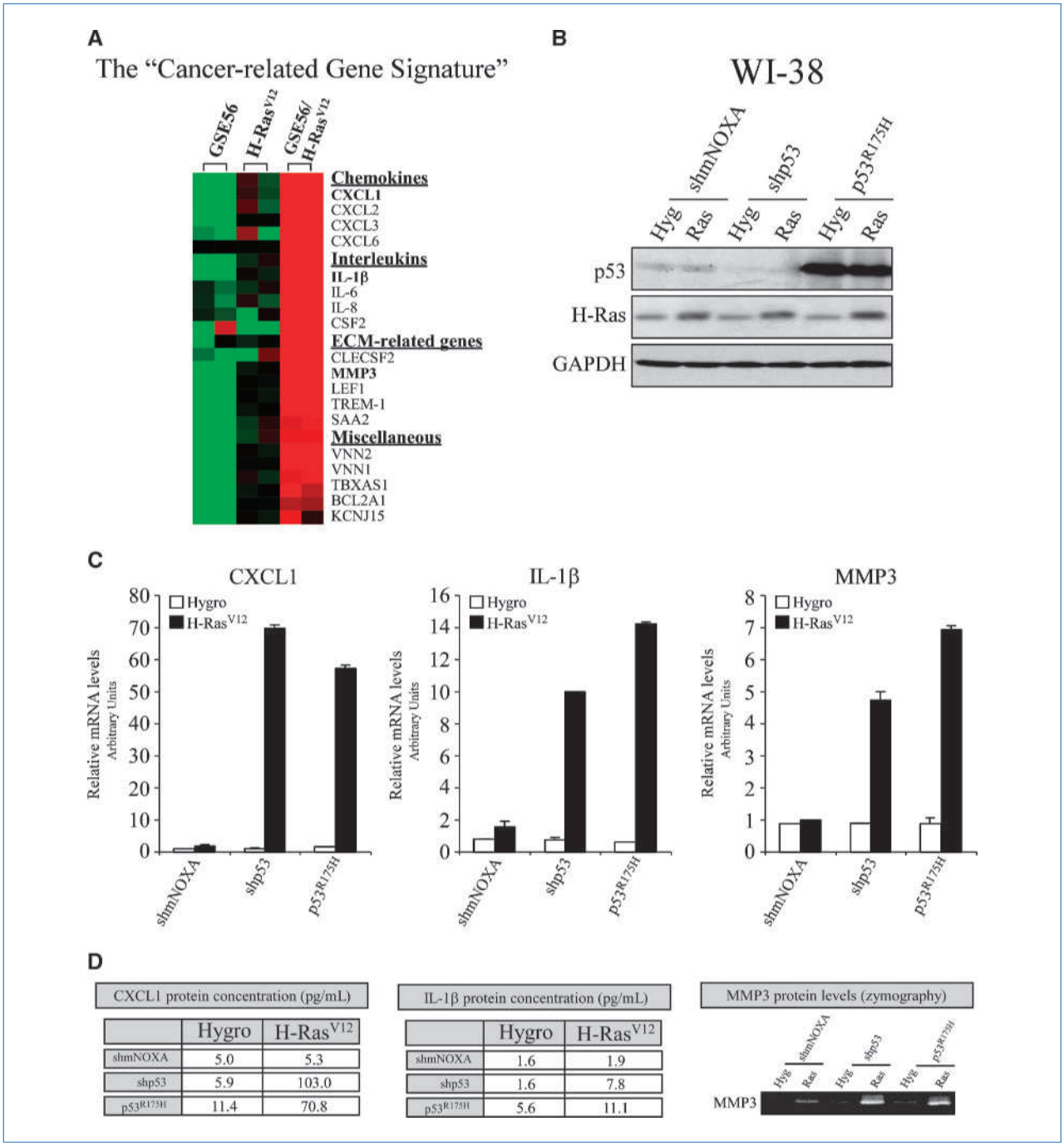

	Hygro	H-Ras^{V12}
shmNOXA	5.0	5.3
shp53	5.9	103.0
p53^{R175H}	11.4	70.8

	Hygro	H-Ras^{V12}
shmNOXA	1.6	1.9
shp53	1.6	7.8
p53^{R175H}	5.6	11.1

Figure 1. p53 inactivation cooperates with H-Ras^{V12} to induce CGS expression. A, the CGS as was previously described (18). Genes marked in bold were selected as representatives. B, Western analysis depicting the protein levels of p53, H-Ras, and GAPDH in the established WI-38 cells. C and D, *CXCL1, IL-1β,* and *MMP3* mRNA levels as measured by QRT-PCR (C) and protein levels as measured by ELISA and zymography (D).

expression of CGS. Ras/shp53 cells were treated with either PD98059 or LY294002 (MAPK and PI3K specific inhibitors, respectively) or with both inhibitors and subjected to CGS mRNA analysis. Western analysis confirmed that the MAPK and the PI3K cascades were significantly attenuated by their specific inhibitors (Fig. 3B). Notably, inhibition of both the MAPK and to a lesser extent the PI3K cascades resulted in reduction in CGS levels (Fig. 3B). These results suggest that at least these two Ras-dependent cascades are involved in the regulation of CGS.

Because the downstream targets of the MAPK and PI3K cascades are c-Jun and NF-κB, respectively, and because their binding sites are enriched in CGS promoters (Supplementary

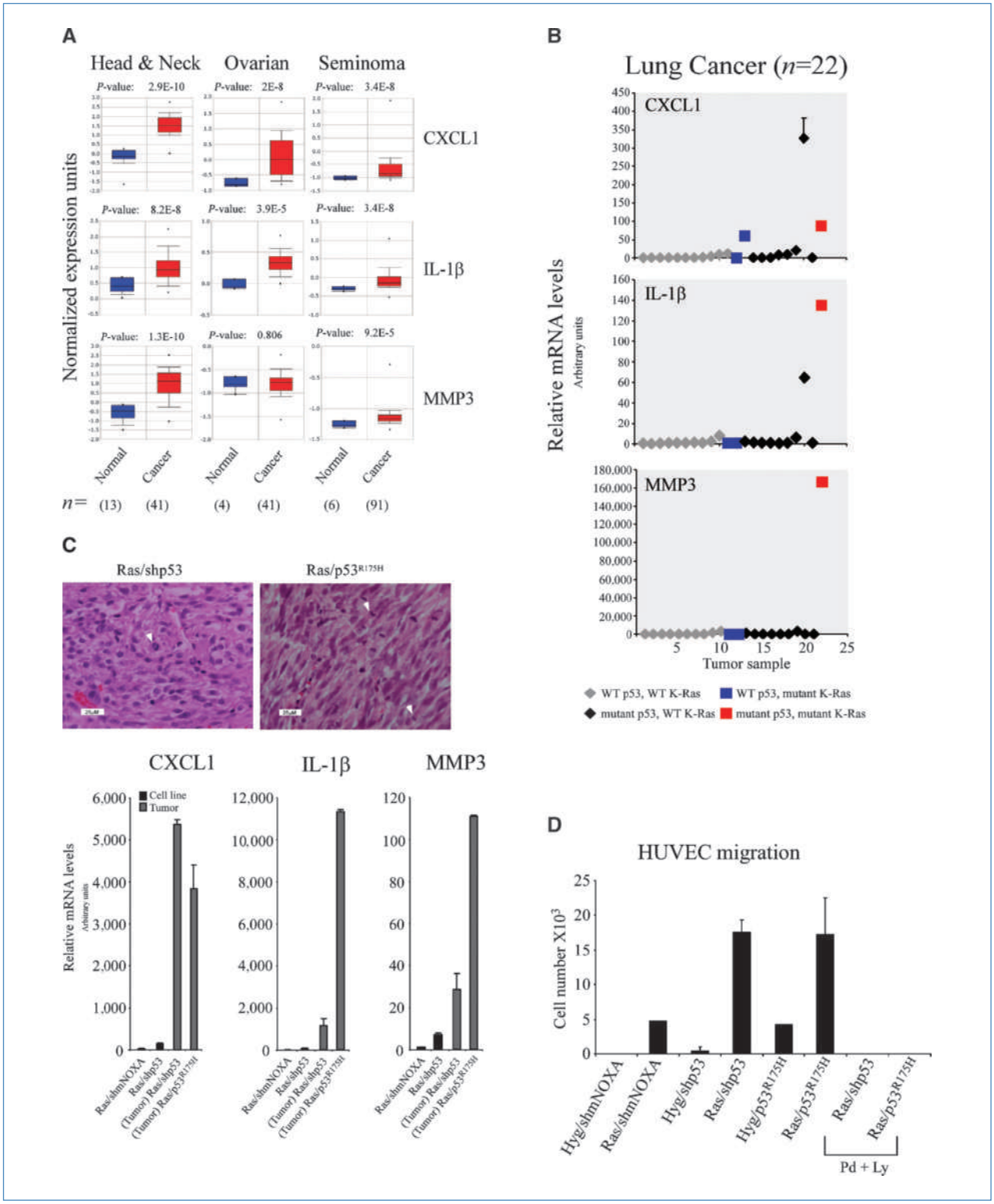

Figure 2. CGS levels are highly correlated with tumorigenicity and with *p53* and *Ras* mutations. A, *in silico* comparison analysis of the CGS expression in normal tissues and tumors using "ONCOMINE" database. B, *CXCL1, IL-1β,* and *MMP3* mRNA levels as measured by QRT-PCR in 22 human lung tumors. C, nude mice were injected with 1×10^7 cells from the indicated cell lines. Top, H&E staining of the generated tumors; white arrows, mitotic cells. Bottom, mRNA levels of *CXCL1, IL-1β,* and *MMP3* as measured by QRT-PCR in the indicated parental cells and in their tumor-derived cells. D, HUVEC cell migration through Transwell after 12 h incubation with conditioned media from the indicated WI-38 cells in basal condition and following PD98059 and LY294002 inhibitors treatment.

Fig. S4), we decided to establish their role in the regulation of CGS to further understand the function of p53 in CGS repression. Therefore, H-Ras^{V12}-expressing cells were stably infected with either empty vector (Neo), c-Jun, or the NF-κB subunit p65 (Fig. 3C; Supplementary Fig. S5). Notably, overexpression of either c-Jun or p65 resulted in significant induction of CGS levels, further supporting the role of H-Ras^{V12} downstream cascades in the regulation of CGS (Fig. 3D). More importantly, the differences in CGS expression between the various p53-expressing cells were abolished following p65 or c-Jun

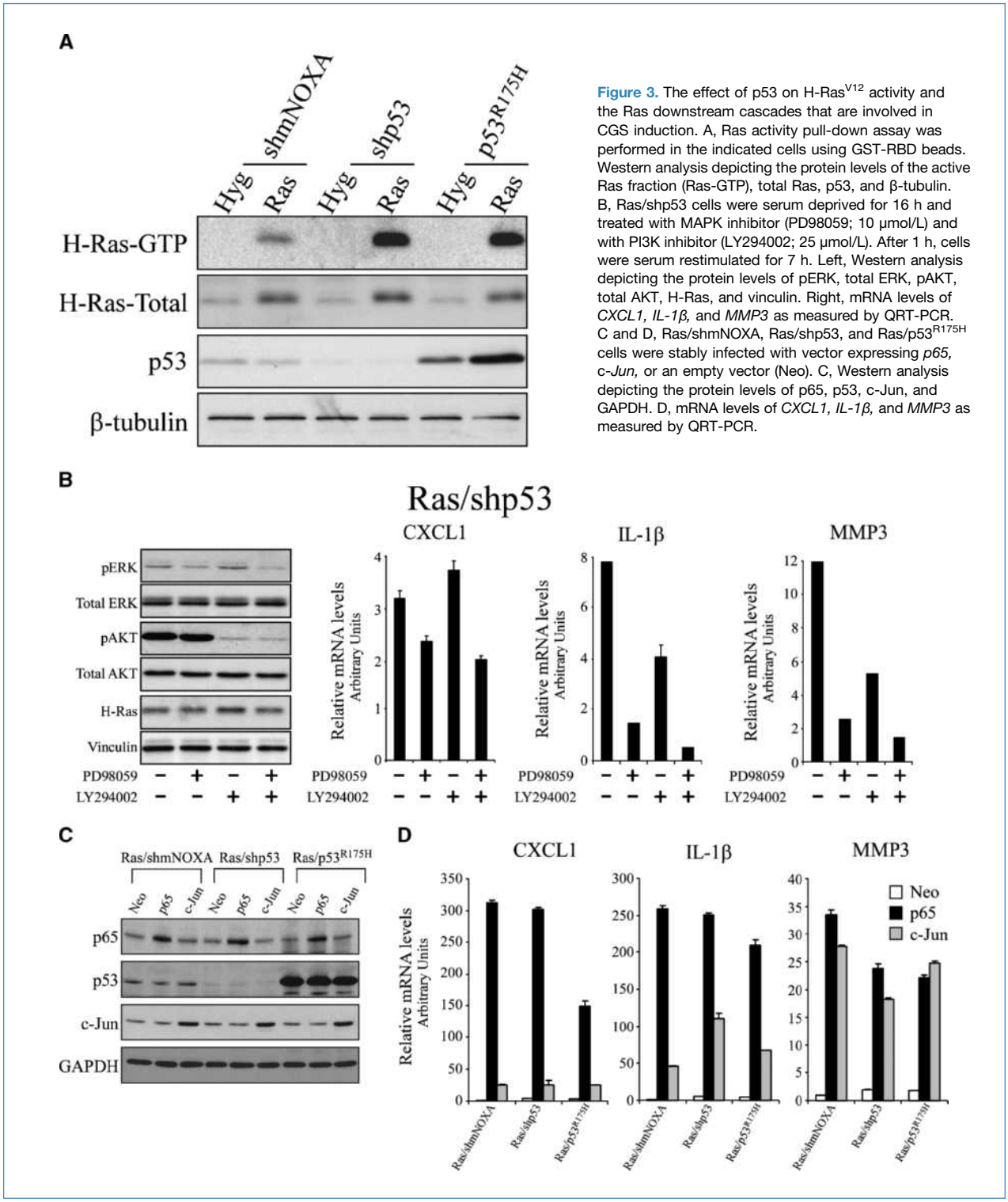

Figure 3. The effect of p53 on H-Ras^{V12} activity and the Ras downstream cascades that are involved in CGS induction. A, Ras activity pull-down assay was performed in the indicated cells using GST-RBD beads. Western analysis depicting the protein levels of the active Ras fraction (Ras-GTP), total Ras, p53, and β-tubulin. B, Ras/shp53 cells were serum deprived for 16 h and treated with MAPK inhibitor (PD98059; 10 μmol/L) and with PI3K inhibitor (LY294002; 25 μmol/L). After 1 h, cells were serum restimulated for 7 h. Left, Western analysis depicting the protein levels of pERK, total ERK, pAKT, total AKT, H-Ras, and vinculin. Right, mRNA levels of *CXCL1, IL-1β,* and *MMP3* as measured by QRT-PCR. C and D, Ras/shmNOXA, Ras/shp53, and Ras/p53^{R175H} cells were stably infected with vector expressing *p65,* c-*Jun,* or an empty vector (Neo). C, Western analysis depicting the protein levels of p65, p53, c-Jun, and GAPDH. D, mRNA levels of *CXCL1, IL-1β,* and *MMP3* as measured by QRT-PCR.

overexpression, indicating the association of p53 in regulating H-Ras^{V12} and its downstream targets. Accordingly, knockdown of p65 resulted in reduced CGS levels (Supplementary Fig. S6). These results suggest that the elevation in H-Ras^{V12} activity by p53 inactivation leads to activated MAPK and PI3K cascades and their targets c-Jun and NF-κB resulting in elevated CGS levels.

p53-dependent repression of CGS is mediated by BTG2 and ATF3. Recently, two p53 targets, BTG2 and ATF3, were shown to suppress Ras-induced transformation through the repression of *cyclin D1* expression, thereby inducing growth arrest (15, 16). To examine the possibility that these two genes harbor additional functions in the p53-H-Ras^{V12} cross talk in respect to CGS regulation, we tested whether ATF3 and BTG2 are functional p53 targets both under basal condition and following p53 activation in our system. Interestingly, whereas p53 transactivated *BTG2* under basal condition and following stabilization, *ATF3* was transactivated only following p53 stabilization (Supplementary Fig. S7). Given that, we decided to examine the effect of these targets on CGS regulation.

Our strategy was to either knockdown or overexpress these genes in Ras/shmNOXA and Ras/shp53 cells and to measure changes in CGS expression. First, the efficiency of the siRNAs in reducing ATF3 and BTG2 protein levels was examined in Ras/shmNOXA cells. As no efficient anti-BTG2 antibodies are available, we assessed the efficiency of BTG2 siRNA in a system wherein BTG2 was myc-tagged and stably overexpressed (Fig. 4A). Notably, knockdown of both ATF3 and endogenous BTG2 resulted in a mild reduction in p53 protein levels, suggesting the existence of a feedback loop between these proteins (Fig. 4B).

Examination of CGS levels following siRNA introduction revealed a significant upregulated expression following a reduction of ATF3 or BTG2 in Ras/shmNOXA cells. This elevation reached to the levels of CGS observed in si-LacZ transfected Ras/shp53 cells (Fig. 4C). Importantly, no additive effect was observed when Ras/shmNOXA cells were introduced with both si-BTG2 and si-ATF3, indicating that both genes affect the same pathway.

Because ATF3 and BTG2 exert some feedback loop on p53, it was important to rule out the possibility that ATF3 and BTG2 knockdown upregulated CGS through ap53 repression. Thus, Ras/shmNOXA and Ras/shp53 cells were stably infected with one of the following vectors: myc-tagged BTG2 (myc-BTG2), myc-tagged mutant BTG2S158G (myc-BTG2^{S158G}), which we found to reduce BTG2 stability, ATF3, ATF3 isoform that lacks its leucine zipper domain and therefore cannot bind to DNA (ATF3Δ-Zip; ref. 38), or empty vector (Neo; Fig. 4D and Supplementary Fig. S8). In agreement with the siRNA data, p53 knockdown cells that overexpress either *ATF3* or *BTG2* exhibited significantly reduced CGS levels when compared with each of the corresponding control cells (myc-BTG2^{S158G}, ATF3ΔZip, or Neo; Fig. 4D).

Importantly, no change was observed in the p53 protein levels following overexpression of *ATF3* or *BTG2,* suggesting a role for ATF3 and BTG2 in repressing CGS, which is independent to their ability to regulate p53 stability. In accordance with their ability to repress CGS, cells overexpressing either *ATF3* or *BTG2* exhibited a reduced colony formation capability (Supplementary Fig. S9). Taken together, these results suggest that both BTG2 and ATF3 are mediators of p53-dependent CGS suppression.

BTG2 interacts with H-Ras^{V12} and reduces its activity. As p53 affects H-Ras^{V12} activity (Fig. 3A) we decided to measure whether BTG2 or ATF3 have an effect on H-Ras^{V12}. First, we examined whether ATF3 or BTG2 bind H-Ras^{V12}. We pulled down and measured the protein levels of both H-Ras^{V12} and p53 from Ras/shmNOXA cell extracts using the GST-ATF3, GST-BTG2, and GST-Empty beads. In agreement with others, we found that ATF3 interacts with p53 but not with H-Ras^{V12} (39). In contrast, BTG2 forms complexes with both p53 and H-Ras^{V12} (Fig. 5A). Accordingly, a reciprocal interaction between BTG2 and H-Ras^{V12} was observed in cells using the LUMIER technique (40) wherein protein-protein complexes are measured by luminescence readout (Supplementary Fig. S10), thus confirming the existence of a specific complex formation between BTG2 and H-Ras^{V12} and prompting the question of whether such interaction affects H-Ras^{V12} activity. Given that, we performed a RBD pull-down assay in Ras/shmNOXA cells, which were transiently introduced with either si-BTG2 or si-LacZ, or in Ras/shp53 cells that overexpress BTG2 that was fused to a luciferase gene or its control vector encoding only to luciferase. In accordance with the elevated CGS levels seen above, knockdown of BTG2 resulted in significant upregulation in H-Ras-GTP levels compared with the si-LacZ cells (Fig. 5B; Supplementary Fig. S11). Accordingly, Ras/shp53 cells expressing luciferase-fused BTG2 exhibited reduced H-Ras-GTP levels compared with their luciferase only control counterparts (Supplementary Fig. S10C). These data show a reciprocal interaction between BTG2 and H-Ras^{V12} and suggest a direct role for BTG2 in repressing H-Ras^{V12} activity. In contrast, ATF3 does not seem to function through a pathway involving complex formation with H-Ras^{V12}.

ATF3 represses CGS expression through direct binding to CGS promoters. Because ATF3 was found to be activated only following p53 stabilization, and both *CXCL1* and *IL-1β* expressions are upregulated following stress (41, 42), we treated Ras/shmNOXA and Ras/shp53 cells with cisplatinum, a DNA damage agent, and measured CGS expression. In agreement with others, we show that treatment of cells with cisplatinum induced CGS levels. However, the induction of CGS was significantly attenuated in p53 cells compared with their p53 K/D counterparts. Importantly, *ATF3* expression was dramatically attenuated in Ras/shp53 cells compared with Ras/shmNOXA cells, suggesting the involvement of ATF3 in the strong inhibitory effect exerted by the stabilized p53 protein (Supplementary Fig. S12).

As ATF3 did not interact with H-Ras^{V12} and the ATF3 isoform ATF3ΔZip that cannot bind DNA did not reduce CGS expression (Fig. 4D), we conclude that ATF3 needs to interact with DNA to exert its function. Because ATF3 was shown to act as a transcription repressor that can interact with either c-Jun or NF-κB (43, 44), key inducer of

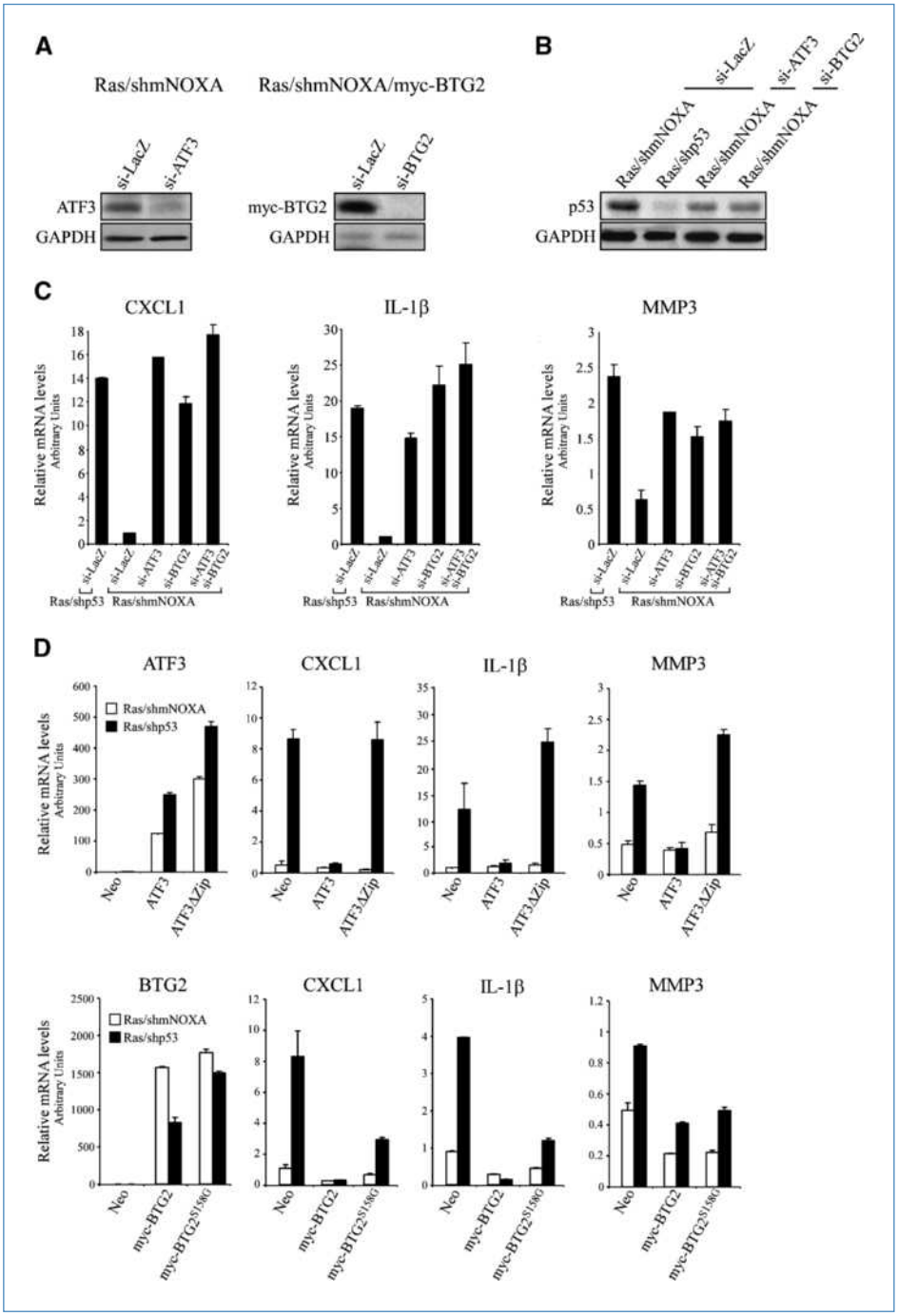

Figure 4. ATF3 and BTG2 negatively regulate CGS expression. WI-38 cells were transfected with siRNAs against ATF3 (si-ATF3), BTG2 (si-BTG2), or LacZ (si-LacZ) as depicted. A and B, Western analysis depicting the protein levels of endogenous ATF3, myc-BTG2, p53, and GAPDH. C, *CXCL1, IL-1β,* and *MMP3* mRNA levels as measured by QRT-PCR. D, Ras/shmNOXA and Ras/shp53 cells were stably infected with one of the following vectors: empty vector (Neo), ATF3, ATF3 isoform (ATF3ΔZip), myc-tagged BTG2 (myc-BTG2), and myc-tagged mutant BTG2 (myc-BTG2^{S158G}). mRNA levels of *CXCL1, IL-1β, MMP3, ATF3, ATF3ΔZip,* and *BTG2* as measured by QRT-PCR.

CGS, we hypothesize that ATF3 represses CGS expression by interacting with one of these factors. Indeed, reciprocal coimmunoprecipitation assays using the Ras/shmNOXA or Ras/shp53 cells overexpressing *ATF3* showed complex formation between ATF3 and c-Jun but not with p65 (Fig. 5C). Therefore we next performed a chromatin immunoprecipitation assay, testing whether ATF3 is able to interact with CGS promoters. Using the Ras/shmNOXA overexpressing *ATF3* cells, we immunoprecipitated ATF3, p53, and transforming growth factor-β (TGF-β) receptor (as a control) and measured the enrichment for *CXCL1, IL-1β,* and *MMP3* promoters in each of the immunoprecipitated proteins. Whereas p53 was found to interact only with its target, $p21^{WAF1}$ promoter, ATF3 was found to interact both with its own promoter and with all three CGS representative gene promoters (Fig. 5D; Supplementary Fig. S13).

Taken together, we discovered a second mechanism for p53-induced repression of CGS, whereas activated p53 upregulates *ATF3*, which in turn interacts with the CGS promoters and represses their expression.

Discussion

Our present study suggests that a cross talk between p53 and activated H-Ras^{V12} plays a pivotal role in regulating the expression of a specific gene cluster of procancerous secreted molecules, the CGS. It should be borne in mind that CGS consists of H-Ras known genes that were shown to play a significant role in the initiation and progression of malignancy (20, 28, 30) and therefore can be regarded as a hallmark for tumorigenicity.

In agreement with that, we found that cells with augmented CGS expression exhibited aggressive transformed phenotypes *in vivo* and a higher efficiency to attract endothelial cells that may suggest a role for CGS in angiogenesis. Of note is the fact that, in mouse-derived tumors, levels of CGS was more pronounced than in their *in vitro* parental lines. To further evaluate the clinical significance of these findings that were derived from *in vitro* and *in vivo* models, we measured the CGS expression levels in 22 human lung cancer samples analyzed for *p53* and *K-Ras* status. In agreement with our model, the highest CGS expression was witnessed in a sample that harbors both mutant p53 and mutant K-Ras. Taken together, our results suggest that CGS can be used in clinic as a readout tool to predict mutations within both *p53* and *K-Ras*, which reflect progressive step in malignancy.

Next, we uncovered several independent pathways, which control the p53-Ras cross talk in conjunction with CGS expression. We found that whereas p53 downregulates the expression of the CGS, mutant p53 or p53 loss upregulated its expression.

entails a complex formation between H-Ras^{V12} and BTG2. BTG2 interacts with H-Ras^{V12} and reduces its GTP loading state.

In accordance with that, it was shown that elevation in H-Ras activity promotes tumorigenicity (45). The mechanism by which BTG2 reduces the levels of the H-Ras-GTP fraction of oncogenic H-Ras^{V12} is not known. Several scenarios can be thought. First, based on the fact that BTG2 is a cofactor that was shown to modulate protein function (46), it can regulate the function of a RasGEF or RasGAP proteins through protein-protein interaction. Second, BTG2 can directly reduce the affinity of GTP to oncogenic Ras. A third scenario is that BTG2 might induce a conformational change in H-Ras^{V12} that facilitates GTP hydrolysis by the mutant Ras. In this sense BTG2 might act like the previously described substrate-assisted catalysis in oncogenic Ras (47). This newly discovered interaction of BTG2 and Ras may explain in part the cooperation between p53 loss and oncogenic H-Ras^{V12}.

A second pathway that may account for the downregulation of CGS by activated p53 is that stabilized p53 upregulates the

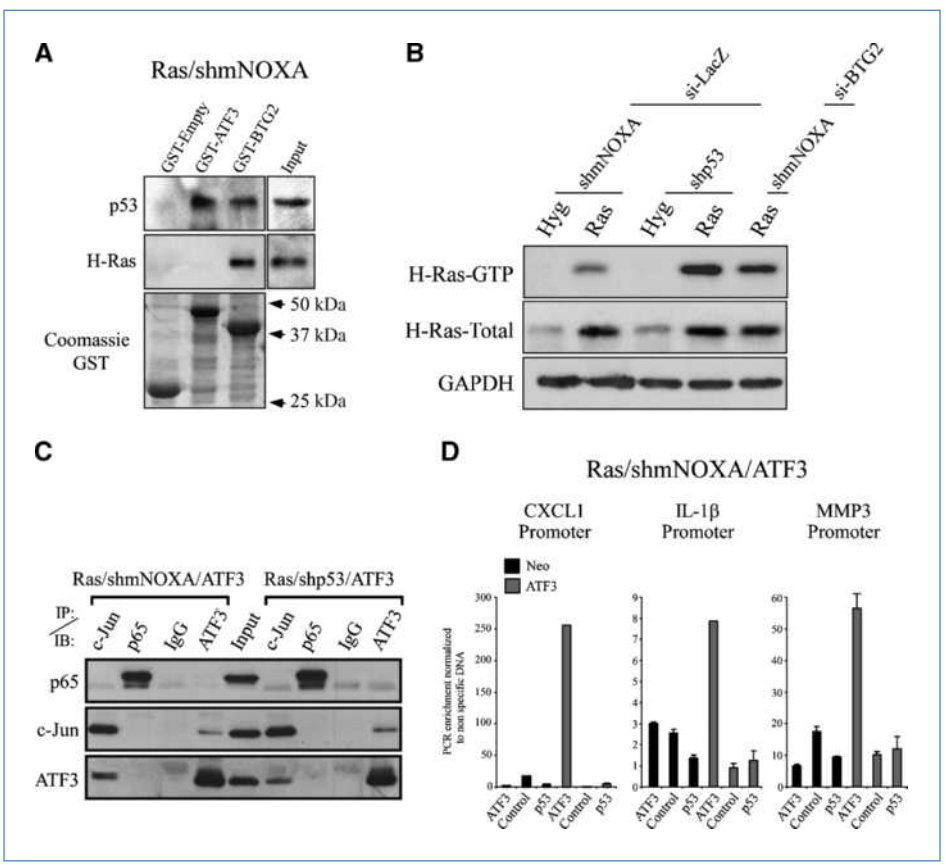

Figure 5. BTG2 and ATF3 way of action in reducing CGS expression. A, a pull-down assay, detecting the protein levels of p53 and H-Ras, was performed in Ras/shmNOXA cells using GST-Empty, GST-ATF3, and GST-BTG2 beads. B, Ras activity assay was performed in the various cells following introduction of the indicated si-RNAs. C, lysates from Ras/shmNOXA and Ras/shp53 overexpressing the *ATF3* gene were immunoprecipitated using c-Jun, p65, ATF3, or IgG antibodies. Western analysis depicting the protein levels of p65, c-Jun, and ATF3. D, chromatin immunoprecipitation was conducted on Ras/shmNOXA overexpressing *ATF3* or empty vector (Neo). Protein-DNA complexes were immunoprecipitated with anti-p53, anti-ATF3, and anti-TGF-β receptor (as a control) antibodies. The amount of precipitated DNA was measured by QRT-PCR with primers directed against the indicated promoters.

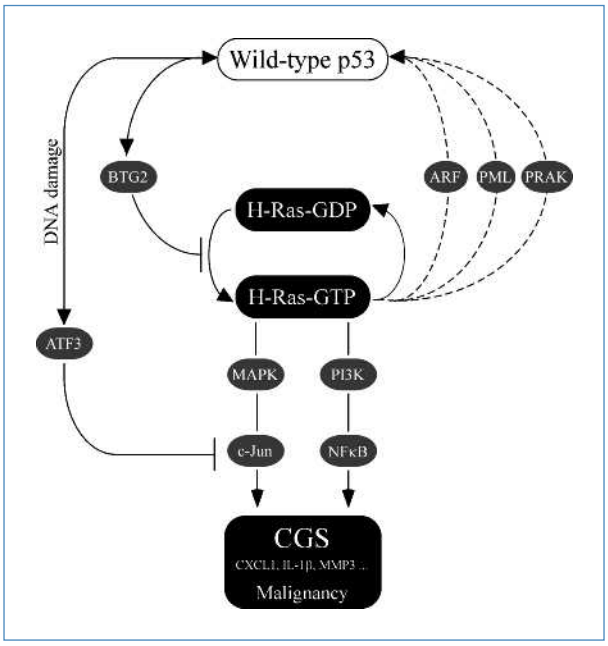

Figure 6. A schematic model describing the suggested p53-H-Ras^{V12} cross talk in the transformation process. Arrows indicate activation, whereas flat-end lines represent repression. Dashed lines indicate literature evidence, whereas continuous lines indicate evidence from the present study.

expression of *ATF3*, which in turn binds directly to DNA sequences contained within the promoters of the CGS, most probably by interacting with the activator protein-1 family member, c-Jun.

In conclusion, we would like to hypothesis that on the H-Ras-CGS genetic axis p53 acts as a negative controller whereas p53 loss or mutant p53 acts as a positive facilitator. This further elucidates the molecular loop between p53 and Ras in which it was already established that p53 protein is stabilized following Ras activation via ARF, DMP1, PML, and PRAK (refs. 48, 49; Fig. 6).

Our working hypothesis is that in precancer cells p53 suppresses the expression of CGS by at least two distinct mechanisms involving transactivation of its target genes *BTG2* and *ATF3*. Inactivation of p53, by any given mechanism, causes a reduction in *ATF3* and *BTG2* expression, resulting in the induction of the H-Ras–dependent CGS expression. The final manifestation of this seems to correlate with the malignant phenotypes, suggesting that CGS may serve as an important hallmark that is regulated concomitantly by the p53 tumor suppressor and the Ras oncogene.

Disclosure of Potential Conflicts of Interest

No potential conflicts of interest were disclosed.

Acknowledgments

We thank Prof. Ronen Alon for advising on the HUVEC migration assay.

Grant Support

Flight Attendant Medical Research Institute Center of Excellence grant, EC FP6 grant LSHC-CT-2004-503576, Yad Abraham Center for Cancer Diagnosis and Therapy, and EC FP7-INFLACARE grant 223151. This publication reflects the authors' views and not necessarily those of the European Community. The EC is not liable for any use that may be made of the information contained herein. V. Rotter is the incumbent of the Norman and Helen Asher Professorial Chair Cancer Research at the Weizmann Institute.

The costs of publication of this article were defrayed in part by the payment of page charges. This article must therefore be hereby marked *advertisement* in accordance with 18 U.S.C. Section 1734 solely to indicate this fact.

Received 07/23/2009; revised 01/07/2010; accepted 01/12/2010; published OnlineFirst 03/02/2010.

References

1. Bos JL. ras oncogenes in human cancer: a review. Cancer Res 1989; 49:4682–9.
2. Hollstein M, Sidransky D, Vogelstein B, Harris CC. p53 mutations in human cancers. Science 1991;253:49–53.
3. Barak Y, Oren M. Enhanced binding of a 95 kDa protein to p53 in cells undergoing p53-mediated growth arrest. EMBO J 1992;11: 2115–21.
4. Momand J, Zambetti GP, Olson DC, George D, Levine AJ. The mdm-2 oncogene product forms a complex with the p53 protein and inhibits p53-mediated transactivation. Cell 1992;69:1237–45.
5. Vousden KH, Lu X. Live or let die: the cell's response to p53. Nat Rev Cancer 2002;2:594–604.
6. Buganim Y, Rotter V. p53: balancing tumour suppression and implications for the clinic. Eur J Cancer 2009;45 Suppl 1:217–34.
7. Vogelstein B, Lane D, Levine AJ. Surfing the p53 network. Nature 2000;408:307–10.
8. Kendall SD, Linardic CM, Adam SJ, Counter CM. A network of genetic events sufficient to convert normal human cells to a tumorigenic state. Cancer Res 2005;65:9824–8.
9. Downward J. Targeting RAS signalling pathways in cancer therapy. Nat Rev Cancer 2003;3:11–22.
10. Parada LF, Land H, Weinberg RA, Wolf D, Rotter V. Cooperation between gene encoding p53 tumour antigen and ras in cellular transformation. Nature 1984;312:649–51.
11. Jenkins JR, Rudge K, Currie GA. Cellular immortalization by a cDNA clone encoding the transformation-associated phosphoprotein p53. Nature 1984;312:651–4.
12. Eliyahu D, Raz A, Gruss P, Givol D, Oren M. Participation of p53 cellular tumour antigen in transformation of normal embryonic cells. Nature 1984;312:646–9.
13. Xia M, Land H. Tumor suppressor p53 restricts Ras stimulation of RhoA and cancer cell motility. Nat Struct Mol Biol 2007;14:215–23.
14. Barbier J, Dutertre M, Bittencourt D, et al. Regulation of H-ras splice variant expression by cross talk between the p53 and nonsense-mediated mRNA decay pathways. Mol Cell Biol 2007;27:7315–33.
15. Lu D, Wolfgang CD, Hai T. Activating transcription factor 3, a stress-inducible gene, suppresses Ras-stimulated tumorigenesis. J Biol Chem 2006;281:10473–81.
16. Boiko AD, Porteous S, Razorenova OV, Krivokrysenko VI, Williams BR, Gudkov AV. A systematic search for downstream mediators of tumor suppressor function of p53 reveals a major role of BTG2 in suppression of Ras-induced transformation. Genes Dev 2006;20:236–52.
17. Milyavsky M, Shats I, Erez N, et al. Prolonged culture of telomerase-immortalized human fibroblasts leads to a premalignant phenotype. Cancer Res 2003;63:7147–57.
18. Milyavsky M, Tabach Y, Shats I, et al. Transcriptional programs following genetic alterations in p53, INK4A, H-Ras genes along

defined stages of malignant transformation. Cancer Res 2005;65: 4530–43.
19. Coppe JP, Patil CK, Rodier F, et al. Senescence-associated secretory phenotypes reveal cell-nonautonomous functions of oncogenic RAS and the p53 tumor suppressor. PLoS Biol 2008;6:e301.
20. McMurray HR, Sampson ER, Compitello G, et al. Synergistic response to oncogenic mutations defines gene class critical to cancer phenotype. Nature 2008.
21. Kogan I, Goldfinger N, Milyavsky M, et al. hTERT-immortalized prostate epithelial and stromal-derived cells: an authentic *in vitro* model for differentiation and carcinogenesis. Cancer Res 2006;66:3531–40.
22. Frangioni JV, Neel BG. Solubilization and purification of enzymatically active glutathione S-transferase (pGEX) fusion proteins. Anal Biochem 1993;210:179–87.
23. Kalo E, Buganim Y, Shapira KE, et al. Mutant p53 attenuates the SMAD-dependent transforming growth factor β1 (TGF-β1) signaling pathway by repressing the expression of TGF-β receptor type II. Mol Cell Biol 2007;27:8228–42.
24. Hoque MO, Begum S, Topaloglu O, et al. Quantitation of promoter methylation of multiple genes in urine DNA and bladder cancer detection. J Natl Cancer Inst 2006;98:996–1004.
25. Ahrendt SA, Halachmi S, Chow JT, et al. Rapid p53 sequence analysis in primary lung cancer using an oligonucleotide probe array. Proc Natl Acad Sci U S A 1999;96:7382–7.
26. Ahrendt SA, Yang SC, Wu L, et al. Comparison of oncogene mutation detection and telomerase activity for the molecular staging of non-small cell lung cancer. Clin Cancer Res 1997;3:1207–14.
27. Jen J, Powell SM, Papadopoulos N, et al. Molecular determinants of dysplasia in colorectal lesions. Cancer Res 1994;54:5523–6.
28. Minn AJ, Gupta GP, Siegel PM, et al. Genes that mediate breast cancer metastasis to lung. Nature 2005;436:518–24.
29. Sternlicht MD, Lochter A, Sympson CJ, et al. The stromal proteinase MMP3/stromelysin-1 promotes mammary carcinogenesis. Cell 1999; 98:137–46.
30. Ancrile B, Lim KH, Counter CM. Oncogenic Ras-induced secretion of IL6 is required for tumorigenesis. Genes Dev 2007;21:1714–9.
31. Lang GA, Iwakuma T, Suh YA, et al. Gain of function of a p53 hot spot mutation in a mouse model of Li-Fraumeni syndrome. Cell 2004;119:861–72.
32. Olive KP, Tuveson DA, Ruhe ZC, et al. Mutant p53 gain of function in two mouse models of Li-Fraumeni syndrome. Cell 2004;119:847–60.
33. Saijo Y, Tanaka M, Miki M, et al. Proinflammatory cytokine IL-1 β promotes tumor growth of Lewis lung carcinoma by induction of angiogenic factors: *in vivo* analysis of tumor-stromal interaction. J Immunol 2002;169:469–75.
34. Wang D, Wang H, Brown J, et al. CXCL1 induced by prostaglandin E2 promotes angiogenesis in colorectal cancer. J Exp Med 2006; 203:941–51.
35. Vojtek AB, Hollenberg SM, Cooper JA. Mammalian Ras interacts directly with the serine/threonine kinase Raf. Cell 1993;74:205–14.
36. Bos JL, Rehmann H, Wittinghofer A. GEFs and GAPs: critical elements in the control of small G proteins. Cell 2007;129:865–77.
37. Scheele JS, Rhee JM, Boss GR. Determination of absolute amounts of GDP and GTP bound to Ras in mammalian cells: comparison of parental and Ras-overproducing NIH 3T3 fibroblasts. Proc Natl Acad Sci U S A 1995;92:1097–100.
38. Chen BP, Liang G, Whelan J, Hai T. ATF3 and ATF3 δ Zip. Transcriptional repression versus activation by alternatively spliced isoforms. J Biol Chem 1994;269:15819–26.
39. Yan C, Lu D, Hai T, Boyd DD. Activating transcription factor 3, a stress sensor, activates p53 by blocking its ubiquitination. Embo J 2005;24:2425–35.
40. Barrios-Rodiles M, Brown KR, Ozdamar B, et al. High-throughput mapping of a dynamic signaling network in mammalian cells. Science 2005;307:1621–5.
41. Chinnaiyan P, Huang S, Vallabhaneni G, et al. Mechanisms of enhanced radiation response following epidermal growth factor receptor signaling inhibition by erlotinib (Tarceva). Cancer Res 2005; 65:3328–35.
42. Reynolds R, Witherspoon S, Fox T. The infant mouse as a *in vivo* model for the detection and study of DNA damage-induced changes in the liver. Mol Carcinogen 2004;40:62–72.
43. Gilchrist M, Thorsson V, Li B, et al. Systems biology approaches identify ATF3 as a negative regulator of Toll-like receptor 4. Nature 2006;441:173–8.
44. Liang G, Wolfgang CD, Chen BP, Chen TH, Hai T. ATF3 gene. Genomic organization, promoter, and regulation. J Biol Chem 1996;271:1695–701.
45. Sun B, Gao Y, Deng L, Li G, Cheng F, Wang X. The level of oncogene H-Ras correlates with tumorigenicity and malignancy. Cell Cycle 2008;7:934–9.
46. Prevot D, Voeltzel T, Birot AM, et al. The leukemia-associated protein Btg1 and the p53-regulated protein Btg2 interact with the homeoprotein Hoxb9 and enhance its transcriptional activation. J Biol Chem 2000;275:147–53.
47. Ahmadian MR, Zor T, Vogt D, et al. Guanosine triphosphatase stimulation of oncogenic Ras mutants. Proc Natl Acad Sci U S A 1999;96:7065–70.
48. McMahon M, Woods D. Regulation of the p53 pathway by Ras, the plot thickens. Biochim Biophys Acta 2001;1471:M63–71.
49. Sun P, Yoshizuka N, New L, et al. PRAK is essential for ras-induced senescence and tumor suppression. Cell 2007;128:295–308.